

RESEARCH

Duodenal L cell density correlates with features of metabolic syndrome and plasma metabolites

Annieke C G van Baar¹, Andrei Prodan², Camilla D Wahlgren³, Steen S Poulsen^{4,5}, Filip K Knop^{3,5,6}, Albert K Groen^{2,7}, Jacques J Bergman¹, Max Nieuwdorp^{2,8,9} and Evgeni Levin^{2,10}

¹Department of Gastroenterology and Hepatology, Academic Medical Center, Amsterdam, the Netherlands

²Department of Vascular Medicine, Academic Medical Center, Amsterdam, the Netherlands

³Center for Diabetes Research, Gentofte Hospital, University of Copenhagen, Copenhagen, Denmark

⁴Department of Biomedical Sciences, Faculty of Health and Medical Sciences, University of Copenhagen, Copenhagen, Denmark

⁵Novo Nordisk Foundation Center for Basic Metabolic Research, Faculty of Health and Medical Sciences, University of Copenhagen, Copenhagen, Denmark

⁶Department of Clinical Medicine, Faculty of Health and Medical Sciences, University of Copenhagen, Copenhagen, Denmark

⁷Department of Laboratory Medicine, University of Groningen, University Medical Center, Groningen, the Netherlands

⁸Department of Internal Medicine, VUMC Free University, Amsterdam, the Netherlands

⁹Wallenberg Laboratory, Sahlgrenska Hospital, University of Gothenburg, Gothenburg, Sweden

¹⁰Horaizon BV, Delft, the Netherlands

Correspondence should be addressed to A C G van Baar: a.c.vanbaar@amc.nl

Abstract

Background: Enteroendocrine cells are essential for the regulation of glucose metabolism, but it is unknown whether they are associated with clinical features of metabolic syndrome (MetS) and fasting plasma metabolites.

Objective: We aimed to identify fasting plasma metabolites that associate with duodenal L cell, K cell and delta cell densities in subjects with MetS with ranging levels of insulin resistance.

Research design and methods: In this cross-sectional study, we evaluated L, K and delta cell density in duodenal biopsies from treatment-naïve males with MetS using machine-learning methodology.

Results: We identified specific clinical biomarkers and plasma metabolites associated with L cell and delta cell density. L cell density was associated with increased plasma metabolite levels including symmetrical dimethylarginine, 3-aminoisobutyric acid, kynurenine and glycine. In turn, these L cell-linked fasting plasma metabolites correlated with clinical features of MetS.

Conclusions: Our results indicate a link between duodenal L cells, plasma metabolites and clinical characteristics of MetS. We conclude that duodenal L cells associate with plasma metabolites that have been implicated in human glucose metabolism homeostasis. Disentangling the causal relation between L cells and these metabolites might help to improve the (small intestinal-driven) pathophysiology behind insulin resistance in human obesity.

Key Words

- ▶ metabolic syndrome
- ▶ incretins
- ▶ enteroendocrine cells
- ▶ plasma metabolites
- ▶ machine-learning methodology

Endocrine Connections
(2018) 7, 673–680

Introduction

The small intestinal mucosa orchestrates a complex response to a range of internal and external stimuli. A pivotal role is played by enteroendocrine cells, whose

dysfunction has been linked to metabolic diseases such as obesity, metabolic syndrome (MetS) and type 2 diabetes (1). The gut incretin hormones, glucagon-like

peptide-1 (GLP-1) and glucose-dependent insulinotropic polypeptide (GIP), produced by enteroendocrine L cells and K cells, respectively, are intimately involved in the regulation of glucose homeostasis (2). The early phase of postprandial GLP-1 secretion is likely mediated by the duodenal L cell population (3, 4). GLP-1 has an important glucoregulatory function and, notably, the incretin effect is reduced in subjects with type 2 diabetes (5). Rerouting of nutrients to L cell-rich parts of the gastrointestinal tract, as seen after gastric bypass surgery, enhances the postprandial GLP-1 responses (6), which in turn – like exogenous administration of GLP-1 receptor agonists (7) – improves glucose tolerance dramatically. L cells have a predominant location in the ileum but are present throughout the small intestine, whereas K cells are primarily located in the duodenum and proximal jejunum (8). On the other hand, somatostatin is produced by delta cells (D cells) in the gastrointestinal tract. Somatostatin reduces gastric acid production and slows down the digestive process by suppressing the release of GIP, insulin and glucagon. To date, it is not clear whether and how the densities of L, K and D cells, respectively, are involved in the regulation of MetS features.

In this cross-sectional study, we aimed to identify plasma metabolites that associate with duodenal L cell, K cell and D cell densities in 38 subjects with MetS. To this end, we used recently published state-of-the-art statistical machine-learning methodology using an adapted version of the elastic net algorithm (9), specifically tailored for identification of the most relevant metabolite biomarkers (10).

Materials and methods

Subjects

We included 38 treatment-naïve obese male subjects with MetS (defined as ≥ 3 out of 5 National Cholesterol Education Program criteria for MetS: fasting plasma glucose ≥ 5.6 mmol/L; triglycerides ≥ 1.7 mmol/L; waist circumference >102 cm; high-density cholesterol <1.03 mmol/L and blood pressure $\geq 130/85$ mmHg). Potential subjects who had a history of cholecystectomy, used a proton pump inhibitor, probiotics or antibiotics in the past 3 months were excluded. The study was approved by the Medical Ethical Committee of the Academic Medical Center Amsterdam in accordance with the Declaration of Helsinki. Written informed consent was obtained from all subjects preceding the screening visit to assess eligibility. During the screening visit, physical

examination was performed to assess height, body weight, waist and hip circumference and blood pressure. Blood was analyzed for hematology parameters, inflammatory markers, liver and kidney function, enzymes, lipids, short-chain fatty acids, gut hormones, glycemic parameters and glucose regulatory hormones. In eligible subjects, a mixed meal test was conducted and on a separate day, a gastro-duodenoscopy was performed where duodenal biopsies were taken. These assessments were performed after an overnight fast.

Mixed meal tolerance test and metabolites

On the morning of admittance, a catheter was inserted into a forearm vein to obtain blood samples during the mixed meal tolerance test. A baseline (fasting) blood sample was taken first. Then, subjects ingested a liquid meal containing 616 kcal/2.6 MJ, containing 61% fat, 33% carbohydrate and protein 6% (11). Blood was sampled for postprandial metabolism at every 30 min for 4 h. These samples were analyzed for glucose, total GLP-1, GIP, peptide YY (PYY), primary and secondary bile acids and triglycerides. The area under the curve and incremental area under the curve were calculated for these parameters for up to 4 h after ingestion of the standardized meal. At baseline, plasma metabolites were determined by liquid chromatography–mass spectrometry for a panel of 96 metabolites containing either amines, oxidative stressors or lipids as previously described (9, 12, 13, 14).

Duodenal biopsy samples

A gastroenterologist at the Academic Medical Center Amsterdam performed a gastro-duodenoscopy to obtain postpapillary duodenal mucosal samples using a biopsy forceps. Biopsy material was immediately fixed in 4% buffered formaldehyde and immersed in this fixative for at least 18 h. After fixation the tissues were embedded in paraffin. These samples were analyzed for histology to exclude structural abnormalities or pathology of the duodenal mucosa. The samples were cut in to sections of 5 μ m and dewaxed through xylene, alcohol and tap water. To retrieve antigens, sections were placed in a 10 mM citrate buffer of pH 6 and boiled in a microwave oven for 15 min. Next, 10-min preincubation in 2% bovine serum albumin was performed ahead of overnight incubation at 4°C with a primary antibody. The following antibodies (mentioned in parentheses) were used for GLP-1 (GLPa, 1F5, 6-2-2006, ‘in-house’

mouse monoclonal, diluted 1:1500), GIP ((1-30)NH₂ (95234-3), 10-4-96 'in-house', rabbit polyclonal, diluted 1:50,000) and somatostatin (somatostatin (1749-6), rabbit, diluted 1:30,000). The sections were incubated for 40 min with a second layer of antibodies to amplify the reaction. Biotinylated secondary immunoglobulins were used (goat anti-rabbit: BA-1000 (Vector Laboratories, Burlingame, CA, USA) for GIP and somatostatin and horse anti-mouse: BA-2000 (Vector Laboratories) for GLP-1; all diluted 1:200). Next, hydrogenperoxide 3% was added to block endogenous peroxidase. The third layer consists of a preformed avidin and biotinylated horseradish peroxidase macromolecular complex (Vector Laboratories, code nr. PK-4000) and was incubated for 30 min. The reaction was developed by the use of 3,3-diaminobenzidine (KEM-EN-TEC Diagnostics, Taastrup, Denmark, cat. no. 4170) for 15 min, followed by 2-min incubation in 0.5% copper sulfate (Merck, art. no. 2790) diluted in Tris buffer 0.05% with Tween 20 (DAKO, S1966). Finally, counterstaining with Mayers Hemalum (Merck) was performed.

The distribution of enteroendocrine cells was evaluated from biopsy slide sections based on immunohistochemical staining (Fig. 1). Digital images of biopsy slides were obtained using Aperio ScanScope scanner with a 20× objective. The newCAST system (Visiopharm, Hørsholm, Denmark) was used to estimate enteroendocrine cell density within the complete individual biopsy slide sections containing both villi and crypts. The size of epithelium and total biopsy area were obtained using a prespecified grid and point-counting technique; the number of +points 'hitting' a structure of interest was multiplied with the area per +point yielding the total area. Next, the number of all immunopositive (stained) cells within the epithelium was counted and divided by the size of the epithelium, thus providing an estimation of cell density.

Statistical analysis

SPSS, version 23 was used to summarize the baseline characteristics of both the subjects and to describe the duodenal biopsies. Continuous variables are summarized utilizing descriptive statistics. An elastic net regularized regression model (15) with stability selection (16) was implemented in Python 2.7 (www.python.org) as a feature selection tool. All data (predictor features as well as the predicted variable) were scaled to zero mean and unit variance. To train each model, the two hyperparameters (the alpha – the size of the regularization penalty and the L1 ratio – the ratio of L1-norm/L2-norm in the model penalty) were optimized using a 5-fold cross-validation procedure on a subset comprising 80% of the data. The model was then tested on the remaining 20% of the data not used in the training. This procedure was repeated 100 times per analysis, each time using different random splitting of the data into training and test subsets. The stability of each feature was calculated as the number of times (out of 100) the respective feature was kept by the model (i.e. the number of times out of 100 runs that the feature had a non-zero regression coefficient). See the architecture of the elastic net model with stability selection workflow in Fig. 2). For each analysis, the top four features with the highest stabilities were selected, providing their stability coefficient was higher than a preset threshold. Stability thresholds were 60% for models using baseline metabolites to predict L cell/K cell/D cell density ('primary models') and 33% for models using fasting plasma measurements and other clinical measurements to predict L cell-linked metabolites ('secondary models'). Permutation testing (1000 permutations) (17) was performed to assess the significance of the link of the selected feature/feature set with the respective predicted variable. Permutation testing was performed by rerunning the model with only the selected features on a random

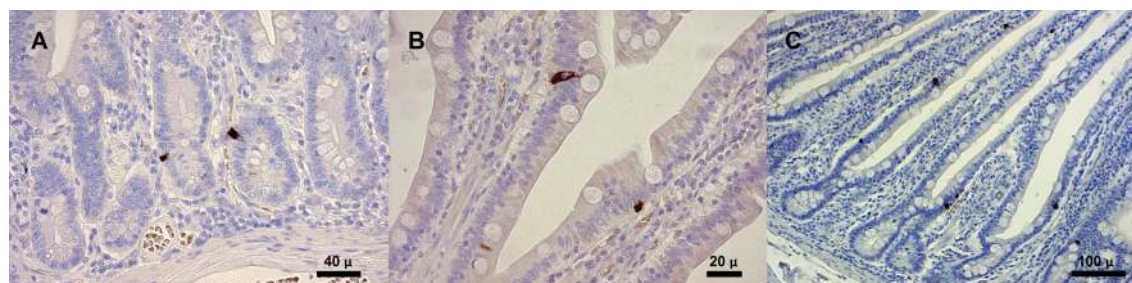


Figure 1

Immunopositive cells stained for (A) GIP (K cells), (B) GLP-1 (L cells) and (C) somatostatin (D cells). GIP, glucose-dependent insulinotropic polypeptide; GLP-1, glucagon-like peptide-1. Scale bar included in each panel separately.

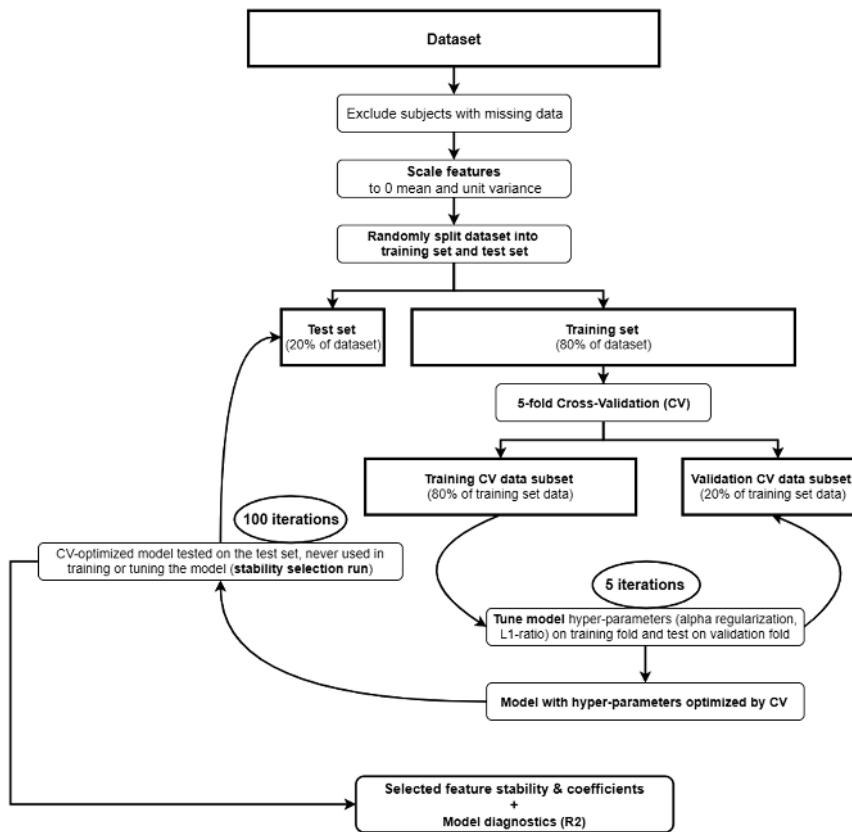


Figure 2
Elastic net flowchart.

train/test data split, and comparing the resulting (true) model R^2 with the (permuted) model R^2 's of 1000 models trained and tested on the same train/test data subsets, with the same hyperparameter ranges as the real model, but with randomly shuffled labels of the predicted variable prior to training. For selected features, the Spearman correlation was calculated between the respective feature and its predicted variable. The detailed architecture of the elastic net model with stability selection workflow is schematically displayed in Fig. 2.

Results

In total, 38 male MetS subjects were included from our previously published study (9) in which we collected duodenal biopsies. All biopsies showed normal histology. Baseline characteristics are shown in Table 1. On average, the mean epithelial area of the duodenal biopsies was $0.66 \pm 0.30 \text{ mm}^2$ and the total area of the biopsies was $1.65 \pm 0.63 \text{ mm}^2$. Mean cell density of K, L and D cells are shown in Table 2. Results of the mixed meal tolerance test (glucose, GLP-1, GIP and PYY) can be appreciated from Supplementary Fig. 1 (see section on supplementary data given at the end of this article).

Upon multivariate modeling using the elastic net model, we found that duodenal L cell density was associated with increased fasting plasma metabolite levels of symmetrical dimethylarginine (SDMA),

Table 1 Subject baseline characteristics.

Subject characteristics	Mean	s.d.	Median	Inter quartile range
Age (years)	54	7	54	8
BMI (kg/m ²)	35	3.6	34.2	5.2
Waist circumference (cm)	121	9	120	14
Systolic blood pressure (mmHg)	145	18	142	23
Diastolic blood pressure (mmHg)	90	12	91	18
HbA1c (mmol/mol)	40	7	40	7
HbA1c (%)	5.8	0.6	5.8	0.6
Fasting glucose (mmol/L)	5.9	0.9	5.6	0.9
Fasting insulin (pmol/L)	121	48	117	46
Total cholesterol (mmol/L)	5.65	1.08	5.48	2.07
HDL cholesterol (mmol/L)	1.15	0.26	1.06	0.36
LDL cholesterol (mmol/L)	3.88	0.94	3.80	1.75
Triglycerides (mmol/L)	1.45	0.65	1.25	0.69
HOMA-IR	4.53	1.95	4.36	2.18

BMI, body mass index; HbA1c, glycated hemoglobin A1c; HDL, high-density lipoprotein; HOMA-IR, homeostatic model assessment-insulin resistance; LDL, low-density lipoprotein.

Table 2 Characteristics duodenal biopsies.

Duodenal biopsy characteristics	Mean	s.d.	Median	Inter quartile range
Length (mm)	3.47	0.84	3.30	1.08
Area epithelium (mm ²)	0.66	0.30	0.50	0.42
Total area biopsy (mm ²)	1.65	0.63	1.60	1.01
L cell density (cells/mm ² epithelium)	10	8	10	13
K cell density (cells/mm ² epithelium)	57	26	56	34
D cell density (cells/mm ² epithelium)	60	35	55	27

3-aminoisobutyric acid (BAIBA), kynurenine and glycine (model $R^2=0.294$, $P=0.017$). The plasma metabolite SDMA correlated most significantly with L cell density (stability 94%) followed by BAIBA (stability 78%). These plasma metabolites were also significantly associated

with the L cell density individually (Fig. 3). We did not find a significant direct correlation between duodenal L cell density and postprandial GLP-1 levels or clinical MetS features. D cells were linked to fasting BAIBA levels (Spearman correlation 0.38, $P=0.0499$, stability 62%). In contrast, we found no associations between duodenal K cell density and circulating metabolites.

We subsequently divided our study subjects based on duodenal L cell density tertiles and found that indeed the upper tertile displayed the strongest correlation with the abovementioned metabolites (Fig. 3).

We then studied the relation between the discovered biomarker plasma metabolites (SDMA, BAIBA, kynurenine and glycine) and duodenal incretin-producing cells and clinical markers. SDMA correlated significantly with plasma creatinine levels (model $R^2=0.224$, $P=0.019$). We found a negative correlation between kynurenine

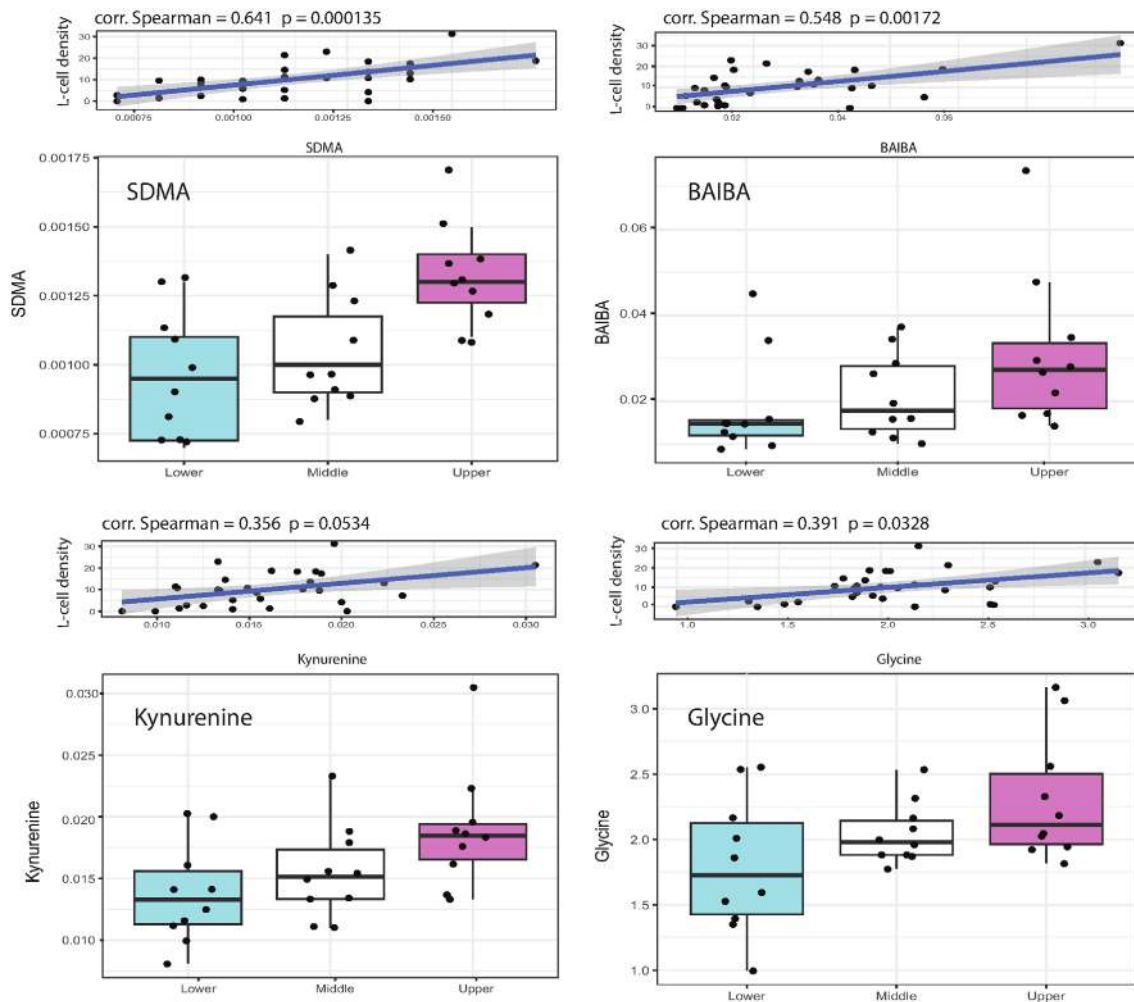


Figure 3

L cell-linked metabolites. Scatterplots with L cell density (cells/mm² epithelium) on x-axis and metabolite quantification on y-axis with depicted below the boxplots with classification by L cell density tertiles and metabolite quantification on y-axis.

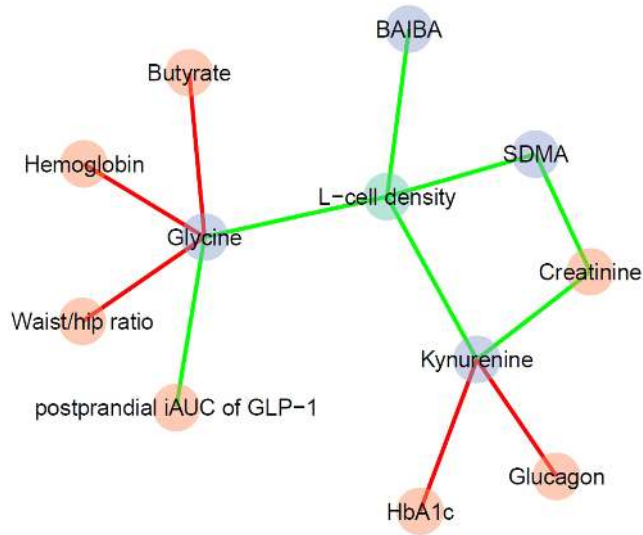


Figure 4
Correlation network with L cells (green), clinical MetS characteristics (pink) and plasma metabolites (blue). Red lines indicate a negative correlation between the two connecting variables. Green lines indicate a positive correlation. BAIBA, 3-aminoisobutyric acid; SDMA, symmetrical dimethylarginine; iAUC, incremental area under the curve; GLP-1, glucagon-like peptide-1; HbA1c, glycated hemoglobin A1c.

and glucagon and glycated hemoglobin (HbA1c), but a positive correlation with kynurenine and creatinine (overall model $R^2=0.353$, $P=0.004$). Glycine was negatively associated with hemoglobin, butyrate and waist-hip ratio. The postprandial GLP-1 response (incremental area under the curve) correlated with glycine with 85% stability (model $R^2=0.514$, $P=0.024$). We found no significant correlation with BAIBA and clinical characteristics. These links are schematically represented in Fig. 4. Except GLP-1, we found no other links between postprandial hormone levels and the discovered biomarker plasma metabolites.

Discussion

In this study, we show that enteroendocrine cell density in the epithelium of the duodenal mucosal varies between subjects with MetS and associates with specific fasting plasma metabolites and markers of glucose homeostasis. In turn, L cell-linked metabolites correlate with clinical features of MetS in our study population. Despite being much more numerous in the duodenum, we found only a single metabolite correlating with D cells and no correlation between K cells and plasma metabolites. Analysis describing duodenal L, K and D cell density indices and correlating these to circulating metabolites

and features of MetS have never been published before to our knowledge. Our findings indicate a link between duodenal L cells and metabolites and clinical features of MetS. We discover that SDMA, BAIBA, kynurenine and glycine together are linked to L cell density, as shown by rigorous multivariate analysis of the data. Below, we hypothesize on mechanisms relating L cell density to the observed clinical and metabolite parameters in MetS (links in Fig. 4).

L cell density correlated strongest with SDMA. This metabolite was reported to decrease in subjects with poor glycemic control (18). In our study, we found a positive correlation between SDMA and duodenal L cell density, which indicates that both SDMA and duodenal L cell density increase in subjects with improved glycemic control. SDMA is eliminated via the kidneys (18), which explains the correlation with plasma creatinine levels observed in our study.

Similarly to SDMA, BAIBA is also associated with improved glycemic control since BAIBA administration improves glucose tolerance (19). We found higher fasting plasma levels of BAIBA in subjects with higher L cell and D cell density but, in contrast to earlier reports, we found no association between clinical features of MetS and BAIBA levels.

Circulating glycine levels are inversely associated with type 2 diabetes risk (19) and plasma glycine levels rise with improved glucose homeostasis (20). As in the case of SDMA and BAIBA, subjects with high glycine levels are metabolically healthier than subjects in which levels of this metabolite are low. Since SDMA, BAIBA and glycine correlated with L cell density, a higher L cell density may be associated with ameliorated glycemic control. At the same time, the hypothetical possibility of dysfunctional L cells cannot be ignored.

We found a negative association between glycine and hemoglobin and waist-hip ratio. Subjects with type 2 diabetes and MetS have higher hemoglobin levels due to increased iron absorption (21). Higher L cell density and higher glycine levels indicate a healthier phenotype, supported by lower hemoglobin levels and lower waist-hip ratio. The postprandial GLP-1 response was linked to glycine, which in turn correlated with L cell density. This finding supports the importance of L cells, especially in subjects with MetS. Interestingly, we found a negative correlation between plasma glycine and butyrate levels. Plasma butyrate levels are usually decreased in MetS subjects due to a lower amount of intestinal butyrate production (22). Since the L cell density-linked metabolite glycine is reported to be

higher in subjects with improved glucose homeostasis, we suggest that the duodenal L cell density increases to compensate for MetS metabolic impairment, as reflected by a decreased butyrate level. This might in turn cause a rise in SDMA, BAIBA and glycine levels, the aforementioned markers of improved glycemic control. We did not find direct links between L cell density and postprandial GLP-1 levels or L cell density and clinical MetS characteristics. This is possibly attributable to the relatively small and homogeneous study population and the cross-sectional nature of this study. Although we did not demonstrate such links with L cell density in our cross-sectional study, it is still possible that L cell density increases following deterioration of MetS, which can in turn improve glycemic control. However, such a series of events can only be detected by taking multiple duodenal biopsies in the course of deterioration (or improvement) of MetS.

Kynurenine was previously found to be increased in subjects with obesity and type 2 diabetes. Kynurenine overproduction is induced by chronic inflammation, one of the mechanisms promoting development of type 2 diabetes (23). We found a positive correlation between duodenal L cell density and kynurenine. Proliferation of L cells may be a physiological response to compensate for the disadvantageous effects of chronic inflammation, as indicated by the correlation between L cell density and kynurenine levels in our study. The negative correlation between kynurenine and HbA1c and glucagon in this study can be due to a kynurenine-driven induction of L cell proliferation, which could potentially improve glycemic control (23). Moreover, it would be interesting to be able to increase the duodenal L cell density or to amplify L cell activation (4) *in vivo* (e.g. using organoids) with the aim of improving glucose regulation. This might also include procedures aimed at specific activation of the duodenal mucosa (24). Such a procedure would allow us to investigate the causal relationship between duodenal L, K and D cell density, metabolites and improvement or deterioration of MetS and type 2 diabetes. Until then, we conclude that small intestinal incretin-producing cells are involved in human glucose metabolism homeostasis via specific plasma metabolites. Disentangling such relations might help to improve the (small intestinal-driven) pathophysiology behind insulin resistance in human obesity.

Supplementary data

This is linked to the online version of the paper at <https://doi.org/10.1530/EC-18-0094>.

Declaration of interest

The authors declare that there are no potential conflicts of interest relevant to the research reported.

Funding

M N is supported by a ZONMW-VIDI grant 2013 (016.146.327) and a Dutch Heart Foundation CVON Young Talent Grant 2013 (on which A P is appointed).

Guarantor's statement

Evgeni Levin is the guarantor of this work and, as such, had full access to all the data in the study and takes responsibility for the integrity of the data and the accuracy of the data analysis.

Author contribution statement

A B designed the study (together with M N), analyzed and interpreted the data, performed statistical analysis and drafted the manuscript. A P analyzed data, performed statistical analysis and drafted the manuscript together with A B. C W acquired data and critically revised the manuscript. S P contributed to the study design and performed critical revision of the manuscript for important intellectual content. F K contributed to the study design and performed critical revision of the manuscript for important intellectual content. A G performed study supervision, interpreted the data and performed critical revision of the manuscript for important intellectual content. J B acquired data and performed critical revision of the manuscript for important intellectual content. M N designed the study together with A B, performed study supervision, interpreted the data and performed critical revision of the manuscript for important intellectual content. E L performed study supervision, performed statistical analysis, drafted the manuscript together with A B and A P and performed critical revision of the manuscript for important intellectual content. All authors approved the final version for publication.

References

- Holst JJ, Pedersen J, Wewer Albrechtsen NJ & Knop FK. The gut: a key to the pathogenesis of type 2 diabetes? *Metabolic Syndrome and Related Disorders* 2017 **15** 259–262. (<https://doi.org/10.1089/met.2017.0015>)
- Campbell JE & Drucker DJ. Pharmacology, physiology, and mechanisms of incretin hormone action. *Cell Metabolism* 2013 **17** 819–837. (<https://doi.org/10.1016/j.cmet.2013.04.008>)
- Theodorakis MJ, Carlson O, Michopoulos S, Doyle ME, Juhaszova M, Petraki K & Egan JM. Human duodenal enteroendocrine cells: source of both incretin peptides, GLP-1 and GIP. *American Journal of Physiology: Endocrinology and Metabolism* 2006 **290** E550–E559. (<https://doi.org/10.1152/ajpendo.00326.2004>)
- Sun EW, de Fontgalland D, Rabbitt P, Hollington P, Sposato L, Due SL, Wattchow DA, Rayner CK, Deane AM, Young RL, *et al.* Mechanisms controlling glucose-induced GLP-1 secretion in human small intestine. *Diabetes* 2017 **66** 2144–2149. (<https://doi.org/10.2337/db17-0058>)
- Nauck M, Stockmann F, Ebert R & Creutzfeldt W. Reduced incretin effect in type 2 (non-insulin-dependent) diabetes. *Diabetologia* 1986 **29** 46–52. (<https://doi.org/10.1007/BF02427280>)
- Rhee NA, Vilsboll T & Knop FK. Current evidence for a role of GLP-1 in Roux-en-Y gastric bypass-induced remission of type 2 diabetes. *Diabetes, Obesity and Metabolism* 2012 **14** 291–298. (<https://doi.org/10.1111/j.1463-1326.2011.01505.x>)



- 7 Vilsboll T, Christensen M, Junker AE, Knop FK & Gluud LL. Effects of glucagon-like peptide-1 receptor agonists on weight loss: systematic review and meta-analyses of randomised controlled trials. *BMJ* 2012 **344** d7771. (<https://doi.org/10.1136/bmj.d7771>)
- 8 Jorsal T, Rhee NA, Pedersen J, Wahlgren CD, Mortensen B, Jepsen SL, Jelsing J, Dalbøge LS, Vilmann P, Hassan H, *et al.* Enteroendocrine K and L cells in healthy and type 2 diabetic individuals. *Diabetologia* 2017 **61** 284–294. (<https://doi.org/10.1007/s00125-017-4450-9>)
- 9 Kootte RS. Improvement of insulin sensitivity after lean donor fecal microbiota transplantation in metabolic syndrome subjects is associated with baseline intestinal microbiota composition. *Cell Metabolism* 2017 **26** 611.e6–619.e6. (<https://doi.org/10.1016/j.cmet.2017.09.008>)
- 10 Botschuijver S, Roeselers G, Levin E, Jonkers DM, Welting O, Heinsbroek SE, de Weerd HH, Boekhout T, Fornai M, Masclee AA, *et al.* Intestinal fungal dysbiosis associates with visceral hypersensitivity in patients with irritable bowel syndrome and rats. *Gastroenterology* 2017 **153** 1026–1039. (<https://doi.org/10.1053/j.gastro.2017.06.004>)
- 11 Reijnders D, Goossens GH, Hermes GD, Neis EP, van der Beek CM, Most J, Holst JJ, Lenaerts K, Kootte RS, Nieuwdorp M, *et al.* Effects of gut microbiota manipulation by antibiotics on host metabolism in obese humans: a randomized double-blind placebo-controlled trial. *Cell Metabolism* 2016 **24** 63–74. (<https://doi.org/10.1016/j.cmet.2016.06.016>)
- 12 Fu J, Schoeman JC, Harms AC, van Wietmarschen HA, Vreeken RJ, Berger R, Cuppen BVJ, Lafeber FPG, van der Greef J & Hankemeier T. Metabolomics profiling of the free and total oxidised lipids in urine by LC–MS/MS: application in patients with rheumatoid arthritis. *Analytical and Bioanalytical Chemistry* 2016 **408** 6307–6319. (<https://doi.org/10.1007/s00216-016-9742-2>)
- 13 Noga MJ, Dane A, Shi S, Attali A, van Aken H, Suidgeest E, Tuinstra T, Muilwijk B, Coulier L, Luijckx T, *et al.* Metabolomics of cerebrospinal fluid reveals changes in the central nervous system metabolism in a rat model of multiple sclerosis. *Metabolomics* 2012 **8** 253–263. (<https://doi.org/10.1007/s11306-011-0306-3>)
- 14 Hu C, van Dommelen J, van der Heijden R, Spijksma G, Reijmers TH, Wang M, Slee E, Lu X, Xu G, van der Greef J, *et al.* RPLC-ion-trap-FTMS method for lipid profiling of plasma: method validation and application to p53 mutant mouse model. *Journal of Proteome Research* 2008 **7** 4982–4991. (<https://doi.org/10.1021/pr800373m>)
- 15 Zou H & Hastie T. Regularization and variable selection via the elastic net. *Journal of the Royal Statistical Society: Series B (Statistical Methodology)* 2005 **67** 301–320. (<https://doi.org/10.1111/j.1467-9868.2005.00503.x>)
- 16 Meinshausen N & Bühlmann P. Stability selection. *Journal of the Royal Statistical Society: Series B (Statistical Methodology)* 2010 **72** 417–473. (<https://doi.org/10.1111/j.1467-9868.2010.00740.x>)
- 17 Golland P, Liang F, Mukherjee S & Panchenko D. Permutation tests for classification. In *Proceedings of the 18th Annual Conference on Learning Theory*, pp 501–515. Bertinoro, Italy: Springer-Verlag, 2005. (https://doi.org/10.1007/11503415_34)
- 18 Can A, Bekpınar S, Gurdol F, Tutuncu Y, Unlucerci Y & Dinccag N. Dimethylarginines in patients with type 2 diabetes mellitus: relation with the glycaemic control. *Diabetes Research and Clinical Practice* 2011 **94** e61–e64. (<https://doi.org/10.1016/j.diabres.2011.08.008>)
- 19 Guasch-Ferre M, Hruby A, Toledo E, Clish CB, Martinez-Gonzalez MA, Salas-Salvado J & Hu FB. Metabolomics in prediabetes and diabetes: a systematic review and meta-analysis. *Diabetes Care* 2016 **39** 833–846. (<https://doi.org/10.2337/dc15-2251>)
- 20 Yan-Do R & MacDonald PE. Impaired ‘glycine’-mia in type 2 diabetes and potential mechanisms contributing to glucose homeostasis. *Endocrinology* 2017 **158** 1064–1073. (<https://doi.org/10.1210/en.2017-00148>)
- 21 Jin Y, He L, Chen Y, Fang Y & Yao Y. Association between serum ferritin levels and metabolic syndrome: an updated meta-analysis. *International Journal of Clinical and Experimental Medicine* 2015 **8** 13317–13322.
- 22 Vrieze A, Van Nood E, Holleman F, Salojarvi J, Kootte RS, Bartelsman JF, Dallinga-Thie GM, Ackermans MT, Serlie MJ, Oozeer R, *et al.* Transfer of intestinal microbiota from lean donors increases insulin sensitivity in individuals with metabolic syndrome. *Gastroenterology* 2012 **143** 913.e7–916.e7. (<https://doi.org/10.1053/j.gastro.2012.06.031>)
- 23 Cervenka I, Agudelo LZ & Ruas JL. Kynurenines: Tryptophan’s metabolites in exercise, inflammation, and mental health. *Science* 2017 **357** eaaf9794. (<https://doi.org/10.1126/science.aaf9794>)
- 24 Rajagopalan H, Cherrington AD, Thompson CC, Kaplan LM, Rubino F, Mingrone G, Becerra P, Rodriguez P, Vignolo P, Caplan J, *et al.* Endoscopic duodenal mucosal resurfacing for the treatment of type 2 diabetes: 6-month interim analysis from the first-in-human proof-of-concept study. *Diabetes Care* 2016 **39** 2254–2261.

Received in final form 11 April 2018

Accepted 18 April 2018

Accepted Preprint published online 18 April 2018